Study of Oxide Film Formed in a Pre Cracked CT Specimen of AISI 304L During a Rising Displacement Test in 288ºC Water

Ángeles Díaz-Sánchez[1,2,3] and Víctor M. Castaño[*,3]

[1]*Instituto de Investigaciones Nucleares,* [2]*Doctorado en Ingeniería, Universidad Autónoma de Querétaro, México*

[3]*Centro de Física Aplicada y Tecnología Avanzada, Universidad Nacional Autónoma de México, A.P. 1-1010, Santiago de Querétaro, Querétaro 76000, México*

Abstract: Study of oxide film formed inside the pre crack in a CT specimens during a rising displacement test in high temperature water (288ºC), under environments used in Boiling Water Reactor (BWR): Normal Water Condition (NWC – 200 ppb O_2) and Hydrogen Water Chemistry (HWC – 125 ppb H_2), was realized by scanning electron microscopy (SEM), and X-ray diffraction (XRD). In both cases the oxide film consisted of two layers and was identify as magnetite. In the case of HWC this results are agree with previous reports that mentioned to magnetite as stable phase in reducing conditions; however the presence of magnetite crystals in NWC has not been reported due to the stable phase in oxidant conditions is hematite. This situation permit infer that inside the pre crack of CT specimens the environmental conditions was different with the oxidant bulk, and probably a poor oxygen access and stagnant conditions within the narrow crack, promoted a localized reducing environment that permitted the magnetite formation. Is evident that the crack growth studies should be considered the conditions inside crack because is significantly different.

1. INTRODUCTION

Stress Corrosion Cracking (SCC) in a general term describing stressed alloy fracture that occur by the propagation of cracks in corrosive environments, SCC has the appearance of brittle fracture, yet it can occurred in highly ductile materials like AISI 304L used in internals components of boiling water reactors (BWR). The high levels of oxygen and hydrogen peroxide generated under a operational Normal Water Condition (NWC) in a BWR, promote a Electrochemical Corrosion Potential (ECP) that is enough to initiate and propagate SCC in susceptible materials (+200 mV *vs* SHE) [1]. Changed water chemistry has been the principal solution for mitigate this cracking, and the change included a more reducing environment by application of Hydrogen Water Chemistry (HWC) by injection of gaseous hydrogen to the feedwater (-230 mV *vs* SHE).

One of the most important models to understand the mechanism of SCC in sensitized stainless steels, has been the theory of the slip-dissolution model that is based on mechanic oxide film rupture and localized dissolution along an active path [2]; the oxide film should permit an active dissolution in the crack tip, but an adequate coated protection in the rest of the crack surfaces avoiding a general corrosion process.

It is evident that the properties of passive film playing a key role in the SCC of austenitic stainless steels and by this reason some authors [3-5] have worked in the study of its chemical and physical properties. For NWC hematite has been the typical structure in the film, because is the stable phase in oxygen condition; while in HWC or reducing environment the oxide film has been reported how magnetite. In almost all the cases, the analysis has been done in flat and polish specimens immerses in high temperature water, so in this paper (and try to collaborate with more information to understand the phenomenon) we present the characterization by Scanning Electron Microscopy (SEM) and by X Ray Diffraction (XRD), of oxide film formed in a narrow surface of the pre-cracked CT specimen of AISI 304L during a rising displacement test in normal and hydrogen water conditions to BWR.

2. MATERIALS AND SPECIMEN PREPARATION

CT specimens were machined; using 25.4 mm thick plates of stainless steel 304L with the chemical composition summarised in the Table **1**, and welded by Shielded Metal Arc Welding (SMAW) with E308L-16, according with a Nuclear Welding Procedure Specification of a real shroud. The Heat affected zone of the specimens agreed with the notch of the specimens.

Table 1.　Chemical Composition

C (%)	Cr (%)	Ni (%)	Mo (%)	Mn (%)	P (%)	S (%)
0.035	18.23	8.72	0.134	1.53	0.01	<0.001

The CT specimens were fatigue pre-cracked in air with a maximum K_I = 25 MPa√m and the Rising Displacement Technique (RDT) was carried out in a refreshed autoclave loop which was attached to a servo-hydraulic tensile test machine that loaded the specimens at very low stroke rates under displacement control (1×10^{-9} m*seg^{-1} and 1×10^{-10} m*seg^{-1}). Similarly to the BWR environment, the temperature of the experiments was 288 ± 1 ºC, at a pressure of 8

*Address correspondence to this author at the Centro de Física Aplicada y Tecnología Avanzada, Universidad Nacional Autónoma de México, A.P. 1-1010, Santiago de Querétaro, Querétaro 76000, México; E-mail: castano@fata.unam.mx

MPa; and the demineralised water with a conductivity approximately of 0.1 µS/cm was equilibrated with appropriate mixtures of argon, oxygen and hydrogen to establish the desired water chemistry: NWC with 200 ppb O_2 and HWC with 125 ppb H_2.

Silver-silver chloride reference electrode were used (Ag, AgCl/0.01 M KCl); all specimens were tested under open circuit condition, and potential measures were registered.

According to ESIS P4-92 D when the experiment finished, the CT specimens were again fatigued in air until they were broken open, chemical and morphology analysis of the oxide film formed in the pre-crack zone (See Fig. **1**), was carried out by Scanning Electron Microscopy, and by X-ray Diffraction.
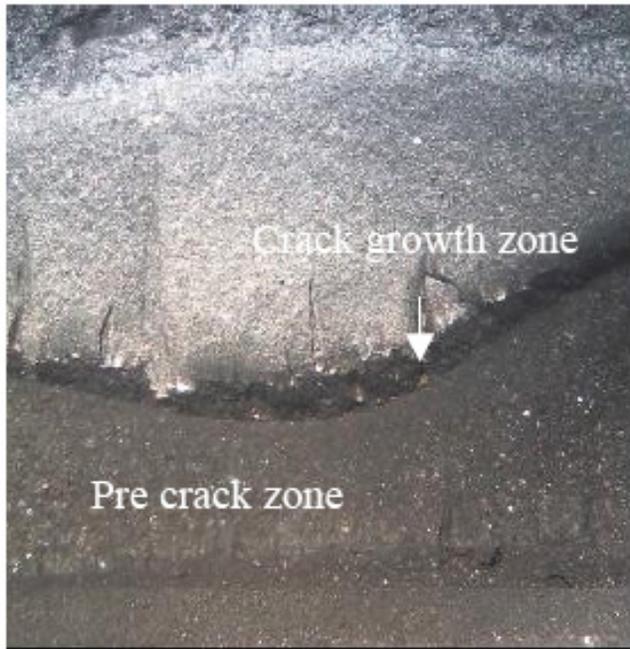
Fig. (1). Oxide film formed in the pre-crack of CT specimen.

3. RESULTS AND DISCUSSION

The experimental conditions of corrosion test performed on the specimens are summarized in Table **2**, included the Electrochemical Corrosion Potential (ECP) that was a typical value in each environment.

Table 2.   Experimental Conditions Summary

Specimen	Displacement Rate m/seg	O_2 or H_2 (ppb) Average	Ecorr *vs* SHE Average	Cond. µS/cm Average
RD24	1×10^{-9}	343 (O_2)	140mV	0.08
RD8	6.6×10^{-10}	270 (O_2)	200mV	0.14
RD20	1×10^{-9}	125 (H_2)	-240mV	0.08

SEM and EDS Analysis

Figs. (**2**, **3**), show scanning electron microscopy micrographs of isometric and well defined particles, that was identify as magnetite. This particles were formed in the pre crack

surface during the Rising Displacement Test under NWC with 200 ppb O_2 and similar that other works [3] the Fig. (**4**), show that the oxide film consisted of two layers: the outer oxide layer with different particle sizes and the inner fine grained layer.
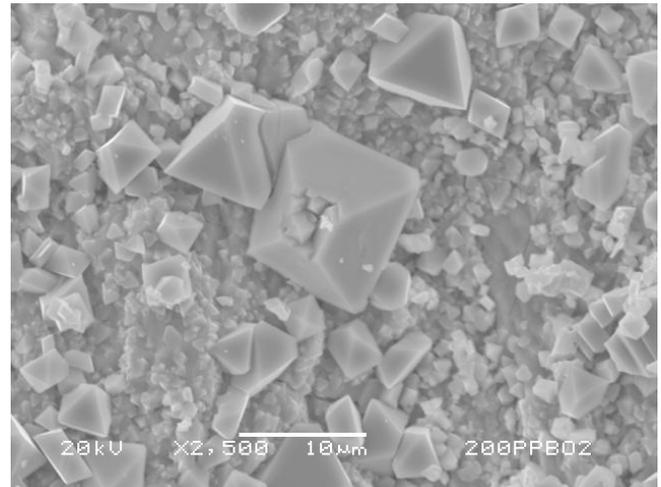

Fig. (2). SEM micrographs showing well defined particles of magnetite.
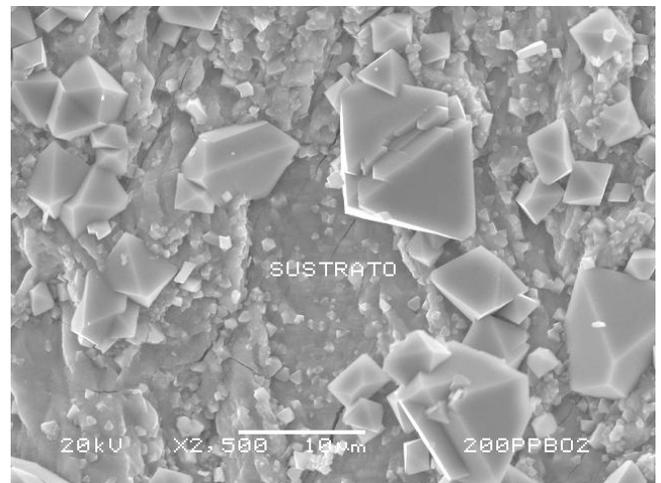

Fig. (3). Particles formed in the pre-crack of the specimens during RDT in NWC.
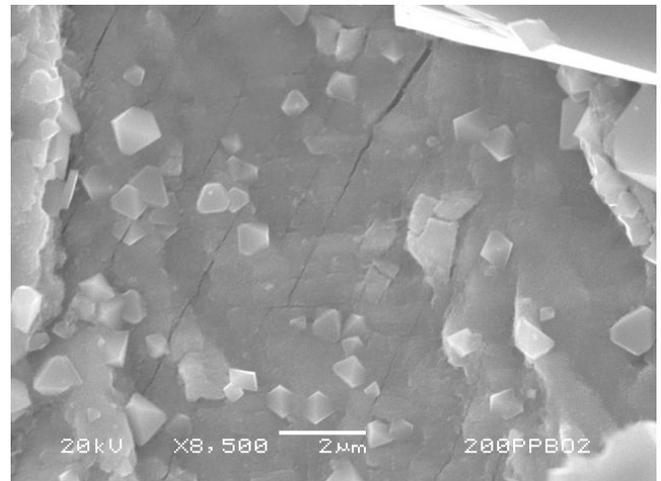

Fig. (4). Picture showing the inner layer formed in NWC.

The average chemical composition on the outer oxide particle and the inner oxide layer was get by punctual EDS and are listed in Table **3**. This results permit to infer that Cr and Ni tends to go into solution and the outer oxide film is poor in this elements; however how has been reported yet, the EDS results on the inner layer show that the level of Cr an Ni is concentrated in this region.

Table 3. Average Chemical Composition on the Outer an Inner Oxide Layers Formed in NWC

	Cr	Fe	Ni
Outer oxide particles	1.17	30.96	0.52
Inner oxide film	17.44	27.97	4.95

In the HWC experimental conditions the outer oxide film formed has smaller particles with a similar shape that the particles formed during NWC (See Figs. **5**, **6**). And in any case can see flat particles that for morphology could be associates with hematite.

Fig. (**7**) shows that under HWC condition there are also two layers and their chemical composition are listed in Table **4**.

Table 4. Chemical Composition on the Outer an Inner Oxide Layers Under HWC

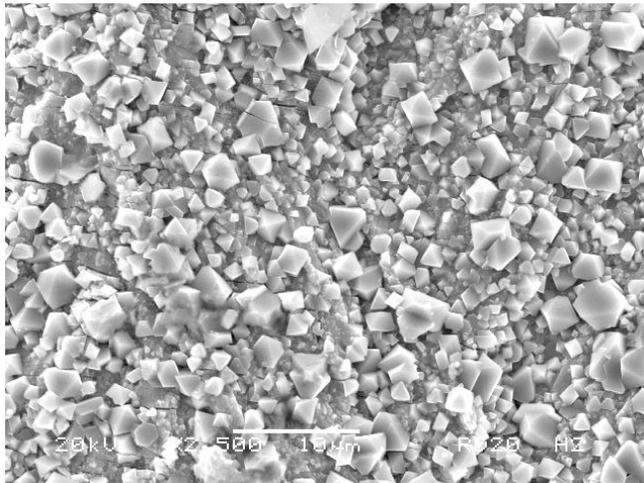|	Cr	Fe	Ni
Outer oxide film	2.44	27.74	2.03
Inner oxide film	14.54	32.34	6.40

Fig. (5). Picture that show smaller particles formed in HWC.

In the same way that the films formed in NWC, the outer layer formed in HWC is poor in Cr and Ni, but tend to concentrates in the inner layer.

X-Ray Diffractometry

Figs. (**8**, **9**) show the X-ray difractograma of the oxide film formed in NWC (200 ppb O_2) and HWC (125 ppb H_2). In both cases and according with the SEM photomicrography evidence, the analyses show the magnetite (Fe_3O_4) presence.
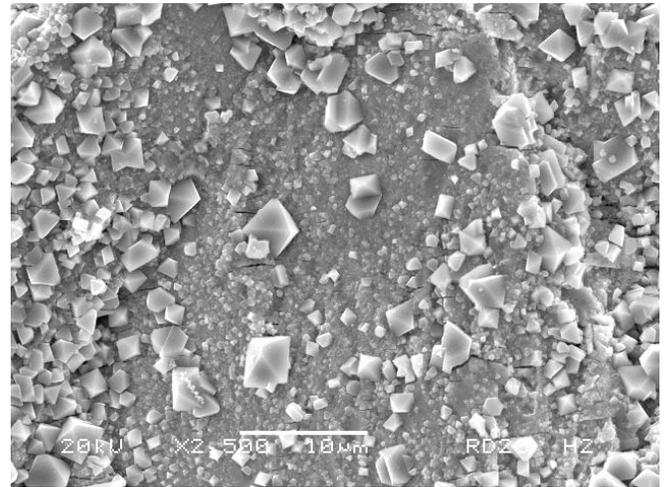

Fig. (6). Particles with a shape associate to magnetite and some of theme with the characteristic shape of hematite.
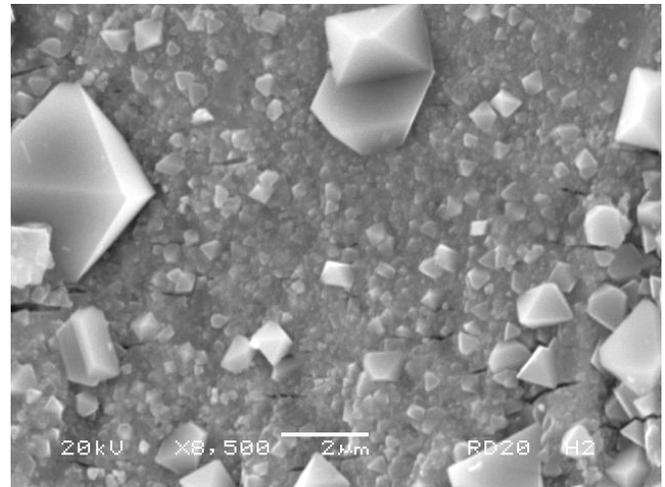

Fig. (7). SEM photomicrography showing the two layers in the pre crack surface formed during HWC conditions.

This results differed from previous reports in which Fe_2O_3 (α-hematite) is the stable form of the film oxide in oxidant environment (200 ppb O_2.) However, considered this crystalline identification and the characteristic shape show in the micrographs can establish that the oxide film formed in the pre crack of the specimen tested in 200 ppb O_2 is magnetite. This situation can explain if we consider that the previous works have been done with flat specimens immerses in the typical environment; however the environmental condition is only controlled in the bulk of the system, and the conditions within a crack can be very different [6]; in fact, is a very well known that in narrow fissures the oxygen access is poor and a stagnant electrolyte solution is present [7]; so this study confirm that the level of oxygen inside the crack is less than the rest of the system.

Fig. (**10**) shows a potential-pH diagrams for iron in supercritical water [6], in which we can see that at potentials above the equilibrium line for Fe_3O_4/Fe_2O_3, both Fe_3O_4 and Fe_2O_3 could exist as metaestable surface phases. And it was likely that the passive film on iron possessed a bilayer structure. However at potentials below this line, but above that for Fe/Fe_3O_4 the passive layer was expected to consist of a single Fe_3O_4 layer. Based on above is not difficult to think in a
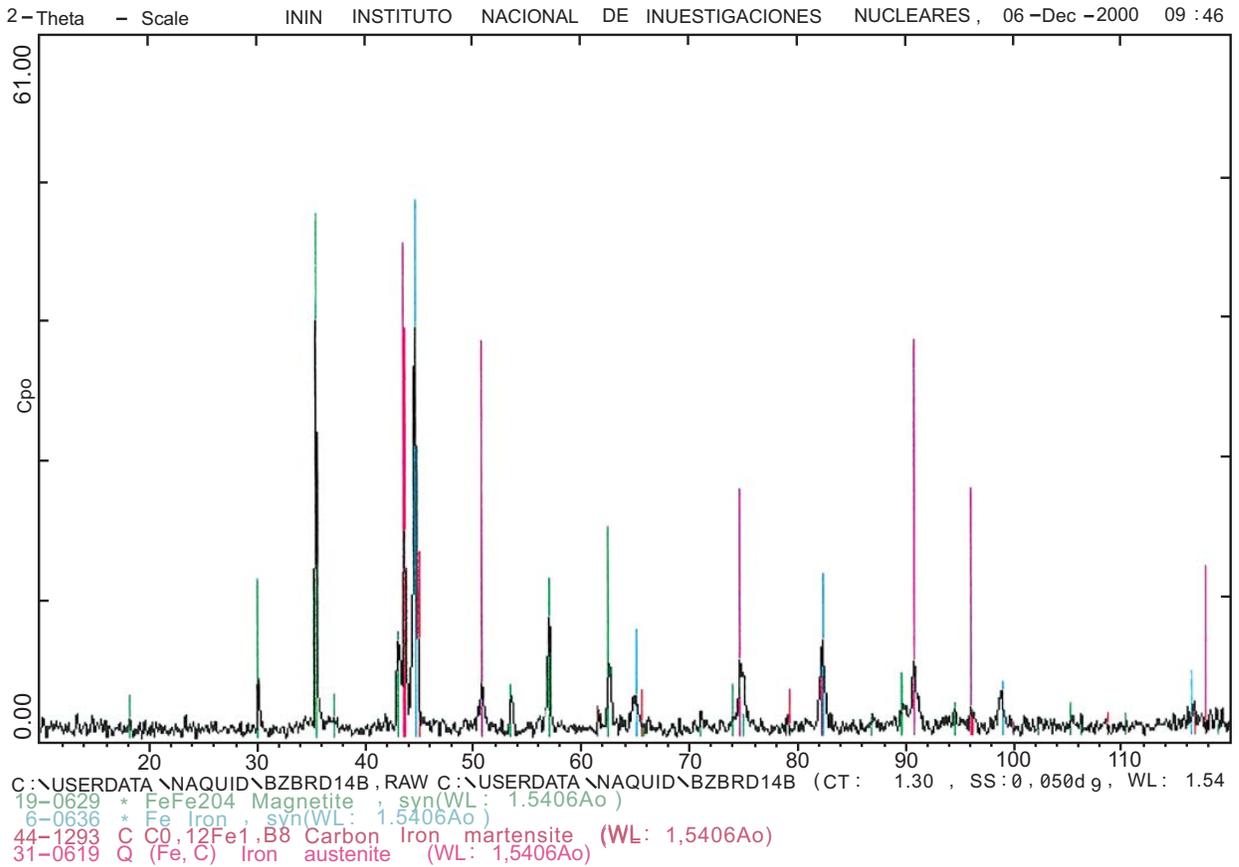
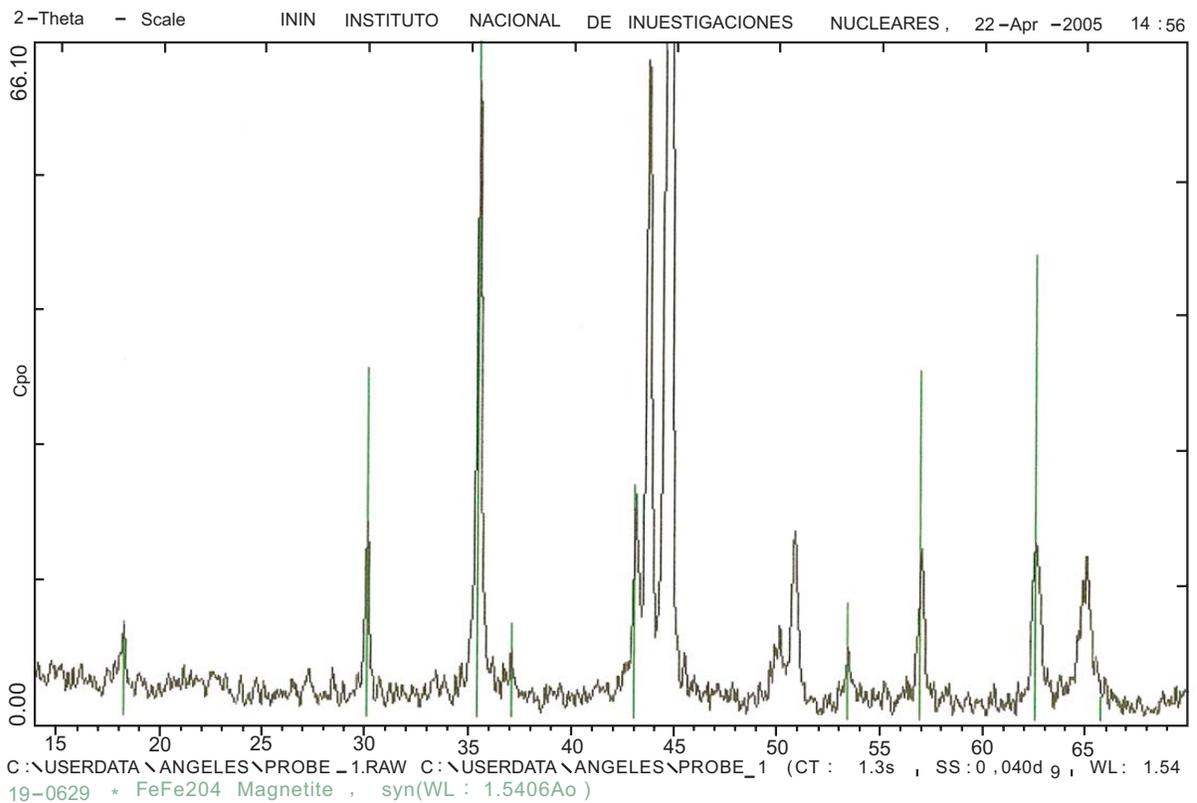**Fig. (8).** XRD patterns of Fe_3O_4 formed in the crack under NWC (200 ppb O_2).

Fig. (9). XRD patterns of Fe_3O_4 formed inside the crack under HWC (125 ppb H_2).

potential reduction inside the crack in which is feasible the magnetite formation or well the existence of the two phases.
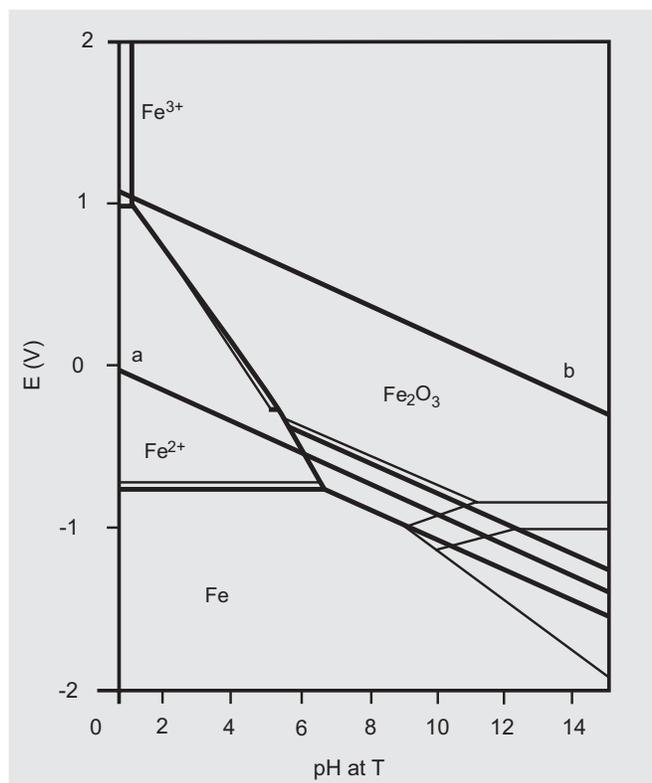

Fig. (10). Potential-pH diagrams obtained by Towsend and Kriksunov (bold lines) at 200ºC [6].

4. CONCLUSIONS

The oxide film formed in NWC and HWC consisted of two layers: the outer oxide layer with different particle sizes and the inner fine grained layer.

In both cases (NWC and HWC), the outer oxide film is poor in Cr and Ni but the inner layer show that the level of Cr and Ni is concentrated in this region.

The surface morphology formed on AISI 304L under NWC and HWC conditions, is typical to magnetite.

By morphology particles of magnetite were presents in the CT surface tested in both conditions.

In both cases (NWC and HWC) the X-ray diffractografy analysis confirm the presence of magnetite (Fe_3O_4) on the outer layer.

This results confirm that the level of oxygen inside the pre crack is less than the rest of the system and under this poor oxygen conditions is feasible the magnetite formation, even though the bulk has and oxidant condition.

REFERENCES

[1] Hettiarachchi S, Cowan RL, Law RJ, Miller WD, Díaz TP. Noble metal chemical addition for IGSCC mitigation of BWRs. Corrosion/99; Paper No. 184, Symposium NACE International, Orange Country Convention Center, Orlando: Florida 1999.

[2] Angeliu TM, Andresen PL, Ford FP. Applying slip-oxidation to the SCC of austenitic materials in BWR/PWR environments. Corrosion/98; Paper No. 262, Symposium NACE International, San Diego: California 1998.

[3] Kim YJ. Analysis of oxide film formed on type 304 stainless steel in 288ºC water containing oxygen, hydrogen and hydrogen peroxide. Corrosion 1999; 5: 81-5.

[4] Kim YJ, Andresen PL. Transformation kinetics of oxide formed on noble metal treated type 304 stainless steel in 288ºC water. Corrosion 2003; 59: 511-9.

[5] Sund G, Molander A. Stress corrosion cracking of prefilmed sensitized type 304 stainless steel in pure water at 250ºC"; Proceedings of the 12th Scandinavian Corrosion Congress Eurocorr´92: Finland 1992.

[6] Kriksunov LB, Macdonald D. Potential-pH diagrams for iron in supercritical water. Corrosion 1997; 53: 605-11.

[7] Betts AJ, Boulton LH. Crevice corrosion: review of mechanisms, modeling, and mitigation. Br Corrosion J 1993; 28: 279-94.